Journal of Solid State Chemistry 232 (2015) 138–143

Contents lists available at ScienceDirect

Journal of Solid State Chemistry

journal homepage: www.elsevier.com/locate/jssc

Effects of indium contents on photocatalytic performance of $ZnIn_2S_4$ for hydrogen evolution under visible light

Kelin Song [a], Rongshu Zhu [a,b,*], Fei Tian [a], Gang Cao [a,b,*], Feng Ouyang [a,b]

[a] Harbin Institute of Technology Shenzhen Graduate School, Shenzhen Key Laboratory of Water Resource Utilization and Environmental Pollution Control, Shenzhen 518055, PR China
[b] Public Platform for Technological Service in Urban Waste Reuse and Energy Regeneration, Shenzhen 518055, PR China

ARTICLE INFO

Article history:
Received 14 May 2015
Received in revised form
8 September 2015
Accepted 22 September 2015
Available online 25 September 2015

Keywords:
$ZnIn_2S_4$
Indium content
Water splitting
Hydrogen evolution
Visible light

ABSTRACT

A series of $ZnIn_xS_{4+y}$ ($x=1.6$, 2.0, 2.3, 2.6, 2.9, 3.1) photocatalysts were synthesized via a facile hydrothermal method and characterized by various analytical techniques, such as XRD, EDS, UV–vis DRS, SEM, TEM, BET and PL. The $ZnIn_xS_{4+y}$ photocatalysts had a similar crystal structure. With the increase of indium content, the absorption edges of $ZnIn_xS_{4+y}$ photocatalysts shifted to longer wavelength, their crystal sizes decreased firstly and then increased and the variation of the specific surface area and total pore volume was exactly opposite. Especially, when $x=2.3$, $ZnIn_{2.3}S_{4+y}$ catalyst had smallest crystal size, largest specific surface area and total pore volume. Additionally, the morphology of $ZnIn_xS_{4+y}$ greatly depended on the contents of indium. The photocatalytic activity of $ZnIn_xS_{4+y}$ was evaluated by photocatalytic hydrogen production from water under visible light. The $ZnIn_{2.3}S_{4+y}$ sample had the highest photocatalytic activity among these $ZnIn_xS_{4+y}$ photocatalysts and its hydrogen production rate was 363 μmol/g h.

1. Introduction

Hydrogen as a clean renewable energy can effectively solve currently energy shortages and environmental pollution caused by fossil fuel consumption. Since the discovery of photoinduced decomposition of water on TiO_2 electrodes in 1972 [1], many studies have been conducted on photocatalytic water splitting to produce hydrogen. In the past few decades, a lot of photocatalysts such as TiO_2-based semiconductors [2–6], $ZnGa_2O_4$ [7], titanates [8,9], niobates [10,11], tantalates [12–14], metal sulfides [15–18], have been developed for water splitting. In these photocatalysts reported, $ZnIn_2S_4$ has recently been studied for its unique optoelectronic [19] and catalytic property [20].

$ZnIn_2S_4$ is the member of the AB_2x_4 family of semiconductors. $ZnIn_2S_4$, which has been proven to have good properties such as suitable band gap corresponding to visible light absorption region, high photocatalytic activity and substantial chemical stability, can act as a catalyst for photocatalytic H_2 evolution [20]. Lei et al. [20] successfully synthesized a novel $ZnIn_2S_4$ photocatalyst and found that $ZnIn_2S_4$ could be used to produce H_2 through water reduction under visible light irradiation, but its hydrogen production efficiency was low. In the past decade, adding additives or doping metals had been shown to improve $ZnIn_2S_4$'s photocatalytic activity. Shen et al. [21] synthesized a series of $ZnIn_2S_4$ photocatalysts via a cetyltrimethylammoniumbromide (CTAB)-assisted hydrothermal method, and found that appropriate amount of CTAB could improve the photocatalytic activity of $ZnIn_2S_4$, and the highest quantum yield at 420 nm of $ZnIn_2S_4$ photocatalyst, which was prepared through the CTAB (9.6 mmol)-assisted hydrothermal procedure for 1 h, was determined to be 18.4%. After that, Shen et al. [22] synthesized a series of alkaline-earth metal doped $ZnIn_2S_4$ photocatalysts and found that the photocatalytic results demonstrated that Ca doping could greatly enhance the activity of $ZnIn_2S_4$, with about two times higher than undoped $ZnIn_2S_4$. The previous study of our group on the rare earth doped catalysts revealed that the La^{3+} showed the best effect [23,24]. Lazzez et al. [25] investigated the structural and optoelectronic properties of In–Zn–S sprayed layers with different $[Zn^{2+}]/[In^{3+}]$ ratios, and found that the $[Zn^{2+}]/[In^{3+}]$ ratios could greatly influence the composition of In–Zn–S thin layers. The film was mainly formed by the ternary compound $ZnIn_2S_4$ which crystallized in cubic phase when $[Zn^{2+}]/[In^{3+}]=0.4$ and the band gap energy increased with the increasing of $[Zn^{2+}]/[In^{3+}]$ ratio. Shen et al. [26] studied the effect of excess zinc on photocatalytic performance of catalyst and synthesized a new series of $Zn_mIn_2S_{3+m}$ ($m=1$–5, integer) photocatalysts by a CTAB-assisted hydrothermal method, and found that photocatalytic performance of catalyst firstly increased and

---

* Corresponding authors at: Harbin Institute of Technology Shenzhen Graduate School, Shenzhen Key Laboratory of Water Resource Utilization and Environmental Pollution Control, Shenzhen 518055, PR China.
E-mail addresses: rszhu@hitsz.edu.cn (R. Zhu), caog@hotmail.com (G. Cao).

http://dx.doi.org/10.1016/j.jssc.2015.09.025

then decreased with the increasing of zinc content, especially when $m=2$, the best photocatalytic performance was obtained. However, the effects of excess indium on photocatalytic performance of $ZnIn_2S_4$ for hydrogen evolution under visible light have rarely been reported.

In order to understand the effects of excess indium on photocatalytic performance of $ZnIn_2S_4$ for hydrogen evolution under visible light, a series of $ZnIn_xS_{4+y}$ ($x=1.6$, 2.0, 2.3, 2.6, 2.9, 3.1) photocatalysts have been successfully synthesized by a hydrothermal route via adjusting the amount of the indium content. We also discussed the characteristics of these photocatalysts, such as crystal size, morphology, optical property and so on in detail.

2. Experimental

2.1. Materials

All chemicals were analytical grade and used as received without further purification. $ZnSO_4 \cdot 7H_2O$, $In(NO_3)_3 \cdot 4H_2O$, TAA (Thioacetamide), absolute ethanol, Na_2S and Na_2SO_3 (purity ≥ 99.99%) were purchased from Sinopharm Chemical Reagent Co., Ltd., China. $H_2PtCl_6 \cdot 6H_2O$ (purity ≥ 99.99%) was purchased from Shanghai July Chemical Co., Ltd., China.

2.2. Preparation of photocatalyst

The $ZnIn_xS_{4+y}$ samples were prepared by a hydrothermal method [27]. For the synthesis of $ZnIn_xS_{4+y}$, 2.56 mmol $ZnSO_4 \cdot 7H_2O$, N mmol $In(NO_3)_3 \cdot 4H_2O$ ($N=4.02$, 5.10, 5.90, 6.70, 7.51, 8.04) and 20.4 mmol TAA were dissolved in 50 mL distilled water. The mixed solution was then transferred into a 100 mL Teflon-lined autoclave. The autoclave was sealed and kept at 160 °C for 1 h, and then cooled to room temperature naturally. A yellow precipitate was obtained, then filtered and washed with absolute ethanol and deionized water for three times. After dried in an oven at 80 °C, a series of catalysts $ZnIn_xS_{4+y}$ were obtained. These catalysts were assigned to $ZnIn_xS_{4+y}$ ($x=1.6$, 2.0, 2.3, 2.6, 2.9, 3.1), respectively.

2.3. Characterization

The UV–visible absorption spectra of the samples were recorded using a UV–vis diffuse reflectance spectroscopy (UV–vis DRS) (UV-2501PC, Shimadzu, Japan) in the spectral range of 300–750 nm. The crystal phases and crystallite sizes of the as-prepared samples were characterized by X-ray diffraction (XRD) (Rigaku, D/max 2500) at room temperature, and the patterns were recorded over the angular range 15–60°(2θ), using a scan rate of 5°/min and Cu-$K_{\alpha 1}$ radiation with working voltage and current of 40 kV and 20 mA, respectively. The surface morphology and energy dispersive spectroscopy (EDS) element mapping of the samples were observed by a field-emission scanning electron microscope with energy dispersive spectrometer (SEM, S-4800, Hitachi, Japan). Elemental analysis was also carried out on an inductively coupled plasma optical emission spectrometer (ICP, OPTIMA 2000DV, Perkin Elmer, USA). Transmission electron microscopy (TEM) and high-resolution TEM (HR-TEM) images were obtained by a Tecnai G2 F30 instrument at an accelerating voltage of 300 kV. The BET surface area was evaluated by N_2 adsorption in a constant volume adsorption apparatus (Bel sorpll, Bayer Japan Co., Ltd., Japan). The analyses of photoluminescence (PL) spectra were carried out at room temperature using a Renishaw in Via raman microscope.

2.4. Photocatalytic reaction

Photocatalytic reactions were conducted in an 868 mL gas-closed stainless steel reactor [28]. The cross section area and height of the reactor were 72.3 cm^2 and 12 cm, respectively. A quartz glass cover on the top of the reactor allowed irradiation to pass through. The light source was a 350-W Xe lamp (Shenzhen Stone-lighting Opto Device Co.,Ltd., China) and the UV part of the light was removed by a cut-off filter ($\lambda > 420$ nm). The light beam was focused coherently on the surface of the 200 mL catalyst suspension (2.8 cm in depth). The suspension in the reactor was continuously stirred using a magnetic stirrer at a speed of 400 rpm. The light intensity was measured using a spectroradiometer (FZ-A, Photoelectric Instrument Factory of Beijing Normal University). In all experiments, 200 mL of deionized water containing 0.2 g of catalyst and 0.25 M Na_2SO_3/0.35 M Na_2S mixed sacrificial agent was added into the reaction cell [21–24,26]. Here, a sacrificial agent was used to scavenge photo-generated holes. In order to remove air prior to the reaction, argon gas was bubbled through the reaction mixture for 30 min before the reaction started. Pt (1 wt%) as a cocatalyst for the promotion of H_2 evolution was photodeposited in situ on the photocatalyst from the precursor of $H_2PtCl_6 \cdot 6H_2O$ [27]. The temperature for all the photocatalytic reactions was kept at 25 ± 1 °C. The concentrations of H_2 were measured with a gas chromatograph (Shanghai Precision & Scientific Instrument Co., Ltd., GC-112A, High-performance carbon molecular sieve packed column (2 m × 3 mm)), equipped with a thermal conductivity detector (TCD). All the measurements of the produced H_2 concentrations at different irradiation times were performed three times to confirm their reproducibility.

3. Results and discussion

3.1. Characterization of catalysts

3.1.1. XRD analysis

Fig. 1 shows the XRD patterns of the $ZnIn_xS_{4+y}$ ($x=1.6$, 2.0, 2.3, 2.6, 2.9, 3.1) samples. $ZnIn_xS_{4+y}$ could be assigned to the crystal phase of hexagonal $ZnIn_2S_4$ (JCPDS No. 65-2023). With the content of indium increasing, a new diffraction peak appears at 33° and gradually increases, which is the (0012) characteristic peak of In_2S_3 [29] (JCPDS No. 65-0459).

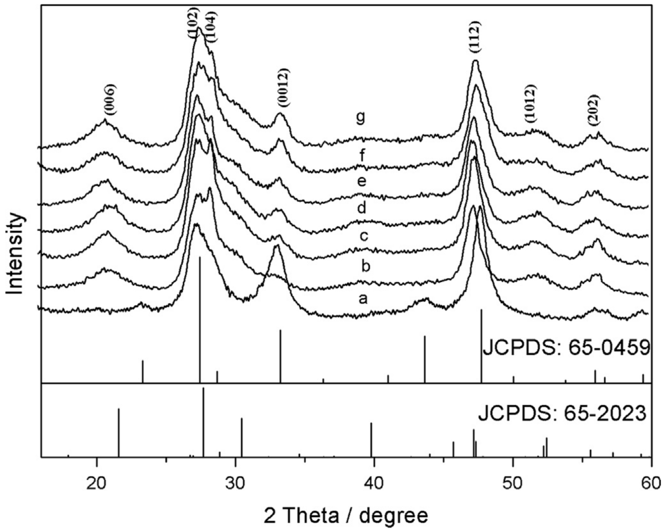

Fig. 1. XRD patterns of $ZnIn_xS_{4+y}$ samples (a: In_2S_3, b: $ZnIn_{1.6}S_{4+y}$, c: $ZnIn_{2.0}S_{4+y}$, d: $ZnIn_{2.3}S_{4+y}$, e: $ZnIn_{2.6}S_{4+y}$, f: $ZnIn_{2.9}S_{4+y}$, g: $ZnIn_{3.1}S_{4+y}$).